

This is the accepted manuscript made available via CHORUS. The article has been published as:

# Retrieval of parameters of few-cycle laser pulses from high-energy photoelectron spectra of atoms by a genetic algorithm

Zhaoyan Zhou, Xu Wang, Zhangjin Chen, and C. D. Lin

Phys. Rev. A **95**, 063411 — Published 13 June 2017

DOI: [10.1103/PhysRevA.95.063411](https://doi.org/10.1103/PhysRevA.95.063411)

# Retrieval of parameters of few-cycle laser pulses from high energy photoelectron spectra of atoms by genetic algorithm

Zhaoyan Zhou,<sup>1,2,\*</sup> Xu Wang,<sup>3</sup> Zhangjin Chen,<sup>4</sup> and C. D. Lin<sup>2</sup>

<sup>1</sup>*Department of Physics, College of Science, National University of Defense Technology, Changsha, Hunan 410073, P. R. China*

<sup>2</sup>*Department of Physics, Cardwell Hall, Kansas State University, Manhattan, Kansas 66506, USA*

<sup>3</sup>*Graduate School, China Academy of Engineering Physics, Beijing 100193, P. R. China*

<sup>4</sup>*Department of Physics, College of Science, Shantou University,*

*Shantou, Guangdong 515063, Peoples Republic of China*

(Dated: May 23, 2017)

According to the quantitative rescattering theory, the laser features are imbedded in the returning electron wave packets. By analyzing high energy photoelectron wave packets on the two sides of the linearly polarization axis we can retrieve the experimental laser pulse irrespective of the atomic targets. Laser parameters including its carrier-envelope phase, pulse duration, and peak intensity can be retrieved within a small range simultaneously from the output of the genetic algorithm. This is a simple direct retrieval method for characterizing a phase-stabilized few-cycle laser pulse based only on one set of photoelectron spectra.

PACS numbers: 32.80.Fb, 32.80.Rm, 42.65.Ky

With the recent progress in laser technology, few-cycle laser pulses are now routinely generated from near-visible to mid-infrared wavelength region. For linearly polarized pulses the time-dependent electric field of a transform limited pulse can be written as  $E(t) = E_L f(t) \cos(\omega t + \varphi)$ , where  $f(t)$  is the field envelope which can be considered to take the form  $\sin^2(\frac{\pi t}{T})$ . Here  $T$ ,  $E_L$ ,  $\omega$  and  $\varphi$  are the pulse duration, field amplitude, carrier frequency and carrier-envelope phase (CEP), respectively. However, except for carrier frequency  $\omega$ , the other three parameters are often not well characterized in each experiment. Today, CEP-stabilized few-cycle laser pulses are already commercially available, but the absolute value of the CEP of the pulse in general is not known. CEP describes the offset of the peak electric field and the peak position of the laser envelope. In principle it can be determined from the response of light-matter interaction in the experiment. For example, due to the CEP, the asymmetric electric field of the laser pulse will result in the asymmetric emission of electrons on the "left" and the "right" directions of the polarization axis. CEP determinations have been suggested based on high-order harmonic generation (HHG)[1, 2], by THz emissions[3, 4], by non-sequential double ionization[5, 6], and by the above-threshold ionization(ATI) electron spectrum[7, 8], *etc.* For analysis of the asymmetry of ATI electrons, in particular, high-energy ATI (HATI) electrons are usually the most common method for CEP retrieval.

The HATI spectrum is often described qualitatively by the classical rescattering model[9, 10]. The electron is first ionized into the continuum and then accelerated in the oscillating electric field. When the laser field reverses its direction the electron may be driven back to recollide with the parent ion and backscatter

to emerge as HATI electrons. If the rescattering is in the forward direction, the resulting low-energy ATI electron would interfere with direct electrons. Such low-energy ATI electrons are harder to treat theoretically since the Coulomb potential plays an important role for its energy distribution[7, 8, 11]. In contrast, for HATI electrons only one or two optical cycles (o.c.) of the field contributes to its spectrum[12–14]. Thus often only HATI spectrum is used to retrieve the CEP since it offers greater contrast in its left-right asymmetry[14] instead of the low-energy ATI electrons[15]. Using the cut-off position of the HATI electrons, the CEP values of few-cycle pulses have been retrieved by comparing theory with experiments[13, 14, 16]. However such a method assumes that the laser duration and intensity are known accurately. In Chen *et al.*[17], it was pointed out that the laser intensity can be determined by the average momentum range of the HATI electrons, while the pulse duration can be determined from the size of the asymmetry ellipse of the HATI spectrum in different energy range. This is a complete characterization method for the temporal structure of the few-cycle laser field and can be used to obtain the CEP value for each laser shot when few-cycle pulses are not CEP-stabilized in the experiment[18]. In other words, in this method experimental data has to be taken from laser pulses covering the whole range of CEP from 0 to  $2\pi$ . In this article, we want to find a way to extract the single CEP value for experiments that are carried out using CEP-stabilized laser pulse.

Experimentally most methods can determine the relative CEP of the pulses, but not the absolute CEP. For the latter, it all relies on comparison with data generated from theory, in particular, those obtained from solving the time-dependent Schrodinger equation (TDSE). In Sayler *et al.*[19], the left-right HATI spectra between Xe and H under the same laser pulse are compared. Based on the TDSE results for atomic hydrogen, the CEPs of the HATI spectra are determined.

---

\*Email address: zhaoyanz@phys.ksu.edu

Generally speaking, one can simulate the ATI spectrum by solving the TDSE[7, 8, 20] or by the strong field approximation(SFA) theory[21, 22]. The former is a quantum calculation and is the most precise simulation method but it is too time consuming since in the iterative retrieval method the ATI spectra would have to be calculated thousands of times by varying the laser parameters. Another approach is the semiclassical second-order SFA (SFA2) theory [23] which treats electron-ion scattering using the plane waves. In the simulation presented here, we take ATI spectrum obtained from solving the TDSE as experimental data and try to retrieve the laser parameters from the "experimental" HATI spectrum through SFA2 simulations. Moreover, to reduce the influence of the atomic potential and raise the accuracy in our simulations, we compare the returning wave packets instead of the photoelectron spectra using the quantitative rescattering (QRS) theory[24, 25]. One can obtain the returning electron wave packets by dividing the differential HATI spectrum by the elastic differential cross section (DCS) such that the retrieved wave packets are independent of targets.

In this paper we used a genetic algorithm (GA) method[26, 27] to reconstruct the few-cycle laser pulse, including its intensity, duration and CEP from a single HATI spectrum. The fitting method is to find the closest match by comparing fitness parameters from the test pulses against the input "experimental" results. By comparing the asymmetry of the wave packet of high energy electrons, we found that the laser pulse parameters can be retrieved within small errors. In the following we first briefly review the QRS theory and then introduce the fitness functions used in the GA. We then show the optimal range of laser parameters that would best reproduce the asymmetry of the HATI spectra.

The wave packet can be extracted from the HATI electron spectrum  $D(p, \theta)$  according to the QRS theory[23–25] by

$$D(p, \theta) = W(p_r) \sigma(p_r, \theta_r), \quad (1)$$

where  $W(p_r)$  is the returning wave packet and  $\sigma(p_r, \theta_r)$  is the elastic DCS. Here  $p_r$  and  $\theta_r$  are the rescattering momentum and angle when the electron first returns to the ion and elastic scattered by the ionic core. Their relationship to  $p$  and  $\theta$  of the measured photoelectron has been explained in detail by Chen *et al.*[23, 24]. For the wave packet along the polarization axis, we can get the right ( $p_z > 0$ ) and left ( $p_z < 0$ ) wave packets from Eq. 1 by  $W_R(p_r) = D(p, \theta = 0)/\sigma(p_r, \theta_r = \pi)$  and  $W_L(p_r) = D(p, \theta = \pi)/\sigma(p_r, \theta_r = \pi)$ . The momentum relation between  $p$  and  $p_r$  can be expressed by  $p = \pm A \mp p_r$  with the upper signs referring to the right side and the lower signs to the left side. For the backscattered returning electron, the relationship between the rescattering momentum  $p_r$  and the vector potential  $A$  at the time of electron's return can be approximated by  $p_r/A \approx 1.25$ [23]. We can get  $p = 1.79p_r$  or  $p = 2.25A$ [17]. In the classical recattering model, the electron is tun-

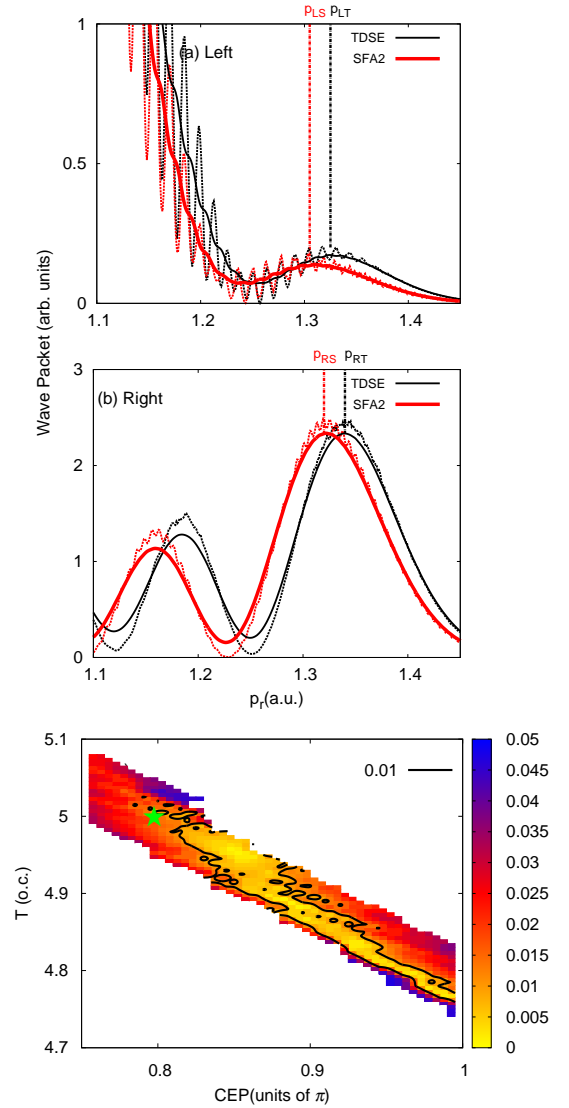


FIG. 1: (a) Left-side ( $z < 0$ ) and (b) Right-side ( $z > 0$ ) wave packets extracted from TDSE (black dashed) and SFA2 (red dashed) for Ar in a 800 nm five-cycle laser pulse at intensity of  $1.3 \times 10^{14} \text{ W/cm}^2$ , for CEP  $\varphi = 0.8\pi$ . To see clearly, the wave packets have been smoothed for both TDSE (black thin, solid) and SFA2 (red thick, solid) results. (c) The fitness parameter calculated from Eq. 2 with different laser duration and CEP. The contour is also set for the small value of  $f_p$  and the green star is the original input data.

nelling ionized near the peak of the laser field and returns to the ion after three quarters of an optical cycle when the electric field is about zero and the vector potential reaches its maximum  $A_0$ [13, 28]. Only considering the outermost portion of the wave packet, its strength is related to the electric field at the tunneling ionization time and its momentum is related to  $A_0$  at the returning time.

The maximum values of the vector potential  $A_0$  in  $\pm z$  directions are usually not equal for a few-cycle laser pulse.

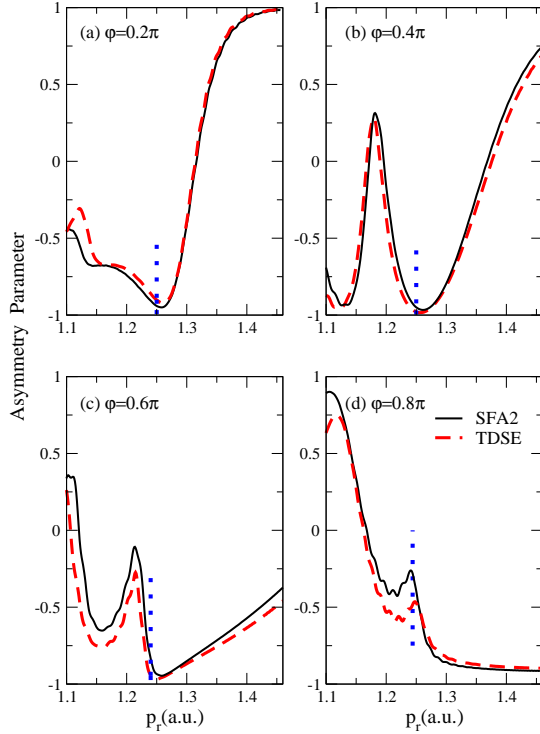


FIG. 2: The corresponding asymmetry parameter calculated from Eq. 3 with TDSE (red dashed) and SFA2 (black solid) method for Ar in a 800nm five-cycle laser pulse at  $1.3 \times 10^{14} \text{W/cm}^2$  for CEP (a)  $\varphi = 0.2\pi$  (b)  $\varphi = 0.4\pi$  (c)  $\varphi = 0.6\pi$  and (d)  $\varphi = 0.8\pi$ . The SFA2 result is shifted to higher momentum by  $\delta p$ .

This difference will lead to asymmetric distribution of the outer wave packet. Figs. 1(a) and (b) are the left and right side wave packets of Ar extracted from the HATI spectrum generated by a 800 nm five-cycle laser pulse at peak intensity of  $1.3 \times 10^{14} \text{W/cm}^2$  for CEP  $\varphi = 0.8\pi$  when the energy of the photoelectron is higher than  $7U_p$ . For such high energy electrons, the wave packets calculated from SFA2 method are slightly shifted lower from the wave packets calculated from TDSE since the SFA2 model neglects the effect of Coulomb force on the electron from the ionic core.

In Fig. 1(a), the dashed lines in black at  $p_{LT}$  and in red at  $p_{LS}$  indicate the peak positions of the left wave packet calculated from TDSE and from the SFA2, respectively. (Recall that TDSE result is treated as the experimental data.) Similar peak momenta of the right wave packet are marked by  $p_{RT}$  and  $p_{RS}$  in Fig. 1(b).

Because  $A_0$  is tuned by the CEP of the laser pulse in both directions, it was suggested [14] that the outermost wave packet evolves smoothly with CEP. This feature can be used as a good criterion for the retrieval of the CEP. The momentum difference of the outermost wave packet on different sides is adopted as the first fitness function,

$$f_p = |\Delta p_{tdse} - \Delta p_{sfa}|, \quad (2)$$

where  $\Delta p_{tdse} = p_{RT} - p_{LT}$  and  $\Delta p_{sfa} = p_{RS} - p_{LS}$  are

the momentum difference of the outermost wave packet calculated from TDSE and SFA2, respectively. We can get a good precision of  $f_p$  to be smaller than  $0.01 a.u.$  when comparing  $\Delta p_{tdse}$  and  $\Delta p_{sfa}$  with the same laser parameter. This means that the effect of Coulomb potential on the peak momenta on the two sides is essentially identical. This simple result works well when we know the pulse duration and intensity.

In reality, in a laser experiment the laser intensity and pulse duration are also not known well. In particular, the intensity will affect the position of the high-energy ATI electron spectra significantly. We thus first calculated the HATI spectra at a few intensities. By comparing the results with experimental data, we can locate the approximate intensity of the laser in the experiment.

We next consider if we know the intensity but we do not know the pulse duration precisely. The contour plot in Fig. 1(c) shows that there is a band on the  $T$  and  $\varphi$  plane where the fitness is less than  $0.01 a.u.$ . For the same laser intensity, a similar vector potential can be obtained when the CEP increases by  $\delta x \times \pi$  while the laser duration is decreased by  $\delta x \times T_{o.c.}$ , where  $T_{o.c.}$  is the optical cycle and  $|\delta x| < 1$ . Thus there is a narrow band of CEP and  $T$  satisfying the criterion of best fitness. To narrow the range of CEP and  $T$  we look for an additional fitness criterion.

The additional fitness we look for is the asymmetry parameter of the wave packets on the two sides. Define the asymmetry of the wave packet at  $p_r$  by

$$A(p_r) = \frac{W_L(p_r) - W_R(p_r)}{W_L(p_r) + W_R(p_r)}. \quad (3)$$

Using the TDSE and the SFA2 methods they are called  $A_t(p_r)$  and  $A_s(p_r)$ , respectively. To calculate the asymmetry from SFA2, we first shift the wave packet on each side to the higher energy by  $\delta p$ , for example, for the right side,

$$\delta p = p_{RT} - p_{RS}. \quad (4)$$

Fig. 2 shows the resulting asymmetry curves from TDSE and from the shifted SFA2. These curves have been smoothed to remove the interference features. For the four different CEPs shown, we note that at each CEP, the asymmetry at the higher momentum region (marked by the vertical dashed lines) typically is monotonic and thus not useful for retrieval. On the other hand, the asymmetry in the lower momentum region shows much pronounced variations, due to the interference of long-versus short-trajectory electrons. They correspond to the second outermost wave packets in Figs. 1(a) and (b). We use a new expression

$$f_a = \int_{p_{r1}}^{p_{r2}} (A_t(p_r) - A_s(p_r))^2 dp_r \quad (5)$$

as the second fitness criterion. The upper momentum is taken at the vertical blue dashed line position and the

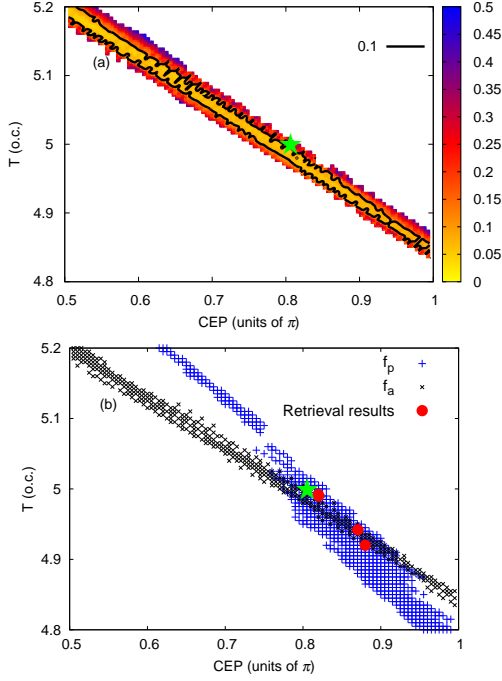


FIG. 3: (a) The fitness parameter calculated from Eq. 5 with different laser duration and CEP. The contour is also set for the small value of  $f_a$  and the green star is the original input data. (b) The small values of  $f_a$  and  $f_p$  within the contour are extracted from (a) and Fig. 1(c). The green star is the original input data. The red dots is the retrieval data of the pulse duration(T) and CEP from GA.

lower limit is taken at the position of the vertical axis. Varying the lower limit does not change the conclusion. Take  $\varphi = 0.8\pi$  as example, this asymmetry fitness parameter is displayed in Fig. 3(a) with different pulse duration and CEP. Clearly there is a band of  $\varphi$  and T that can fall within the chosen fitness value. However, by combining the two fitness plots from Fig. 1(c) and Fig. 3(a), we can locate a small area where the two bands overlap, see Fig. 3(b). This area covers a range of CEP values of less than  $0.1\pi$  and pulse duration of less than 0.05 o.c. (out of 5 o.c.).

For practical purpose, any values of CEP and T combinations within the area would be acceptable. Alternatively we have also tested the method by using GA to identify the CEP and T. We first limit that  $f_p < 0.01 a.u.$ , and use  $f_a$  as the fitness function. The three red points in Fig. 3(b) are the retrieved T and  $\varphi$  after 2000 generations in GA using different initial random seeds. The retrieval values are located within the overlap area.

We have applied the same method to laser pulses with different CEPs, the error ranges for each of the input CEP are shown in Fig. 4. We note that the error is larger near  $\varphi=0.5\pi$ . If we take the middle point of each band, the retrieved error in the CEP is about  $0.1\pi$  and the error in the pulse duration is about 0.1 o.c.. These results are considered to be quite accurate for identifying the

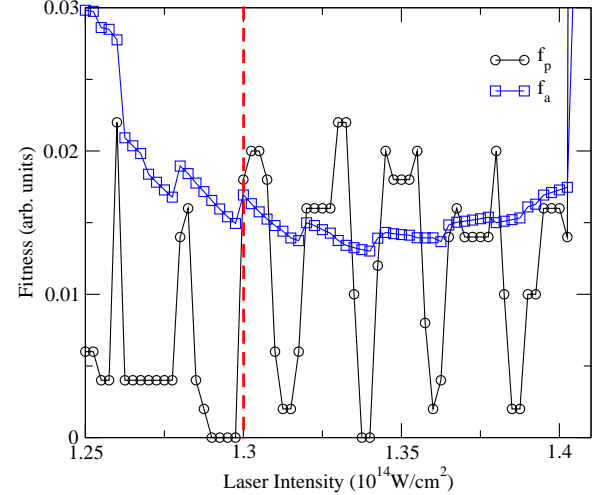
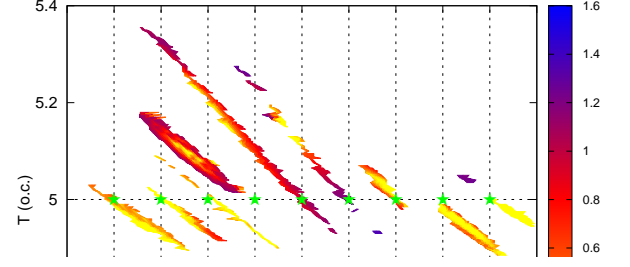


FIG. 5: The fitness parameters vs laser intensities around the input laser intensity  $I = 1.3 \times 10^{14} W/cm^2$  (indicated by the red dashed line) for five-cycle laser pulse with fixed CEP  $\varphi = 0.8\pi$

essential laser parameters in experiments. In particular, there still has no well-accepted method for characterizing the CEP if the laser is already CEP stabilized.

Using the same method we can also retrieve laser intensity within a few percent. Consider the two fitness parameters  $f_p$  and  $f_a$  found above, they would be kept at small values if the laser intensity is close to the original input one when the duration and CEP of the laser pulses are fixed. Fig. 5 shows that the two fitness parameters  $f_p$  and  $f_a$  remain small within the intensity range shown. As the intensity goes out of this range, the fitness deteriorates quickly. Alternatively if we do not fix

TABLE I: The retrieved parameters of laser pulse  $E(t) = \sqrt{I} \sin^2(\frac{\pi t}{T}) \cos(\omega t + \varphi)$  from GA for Ar and Xe with fixed laser wavelength to be 800 nm.

Parameters	$I(10^{14} \text{W/cm}^2)$	T (o.c.)	$\varphi(\pi)$
Input	1.3	5.0	0.8
Output1(Ar)	1.323	5.07	0.722
Output2(Ar)	1.336	5.03	0.778
Output1(Xe)	1.319	4.98	0.797
Output2(Xe)	1.332	4.9	0.877

the laser intensity in the GA retrieval process, the output intensity will change randomly but they remain from  $1.27 \times 10^{14} \text{W/cm}^2$  to  $1.4 \times 10^{14} \text{W/cm}^2$ . In another test we also perform GA with  $E_L, T, \varphi$  as unknown parameters, we were able to retrieve these parameters, shown in Table I that are quite close to the input ones, for the two targets Ar and Xe, for example. These results support that the two fitness parameters introduced in this work allow the retrieval of the values of  $E_L, T, \varphi$  to within a narrow range, based on the asymmetry of one single photoelectron spectrum along the polarization axis of the laser pulse.

In conclusion, we suggest a simple method to characterize the carrier-envelope-phase, the pulse duration and peak intensity of a few-cycle linearly polarized laser pulse. By analyzing the asymmetry of the photoelectron spectra at high energies and compared the outermost and

the second outermost wave packets on the "left" and "right" sides of the polarization axis we proposed two fitness parameters to characterize their asymmetric distributions. Using electron spectra calculated from solving the TDSE as "experimental" data, we used genetic algorithm to identify CEP, pulse duration and peak intensity of the unknown laser pulse to a small error range. The method is simple and uses only one photoelectron spectrum. These parameters can be retrieved within a short time. It is suggested that this method can be implemented in any measurements with few-cycle pulses to replace other means which are often just based on simple estimates. To assure the method works correctly, electron spectra from two atomic targets can be collected in coincidence with the atomic ions. The laser parameters from the two spectra can then be compared to each other.

### Acknowledgments

ZYZ would like to thank the hosting of J. R. MacDonald Laboratory at Kansas State University where this work was carried out. CDL is supported in part by Chemical Sciences, Geosciences and Biosciences Division, Office of Basic Energy Sciences, Office of Science, U. S. Department of Energy under Grant No. DE-FG02-86ER13491. ZJC was supported by the National Natural Science Foundation of China under Grant No. 11274219.

- 
- [1] A. de Bohan, P. Antoine, D. B. Milošević, and Bernard Piraux, Phys. Rev. Lett. 81, 1837 (1998)
  - [2] C. A. Haworth, L. E. Chipperfield, J. S. Robinson, P. L. Knight, J. P. Marangos, and J. W. G. Tisch, Nat. Phys. 3, 52 (2007)
  - [3] M. Kieß, T. Löffler, M. D. Thomson, R. Dörner, H. Gimpel, K. Zrost, T. Ergler, R. Moshhammer, U. Morgner, J. Ullrich, and H. G. Roskos, Nat. Phys. 2, 327(2006)
  - [4] Y. Bai, L. Song, R. Xu, C. Li, P. Liu, Z. Zeng, Z. Zhang, H. Lu, R. Li, and Z. Xu, Phys. Rev. Lett. 108, 255004 (2012)
  - [5] X. Liu, H. Rottke, E. Eremina, W. Sandner, E. Goulielmakis, K. O. Keeffe, M. Lezius, F. Krausz, F. Lindner, M. G. Schätzel, G. G. Paulus, and H. Walther Phys. Rev. Lett. 93, 263001 (2004)
  - [6] Q. Liao, P. Lu, Q. Zhang, W. Hong, and Z. Yang, J. Phys. B: At. Mol. Opt. Phys. 41, 125601 (2008)
  - [7] S. Chelkowski and A. D. Bandrauk, Phys. Rev. A 65, 061802(R)(2002)
  - [8] S. Chelkowski, A. D. Bandrauk, and Alexander Apolonski, Phys. Rev. A 70, 013815 (2004)
  - [9] G. G. Paulus, W. Becker, W. Nicklich, and H. Walther, J. Phys. B: At. Mol. Opt. Phys. 27, L703(1994)
  - [10] P. B. Corkum, Phys. Rev. Lett. 71, 1994 (1993)
  - [11] D. B. Milošević, G. G. Paulus, D. Bauer, and W. Becker, J. Phys. B: At. Mol. Opt. Phys. 39, R203, (2006)
  - [12] D. B. Milošević, G. G. Paulus, and W. Becker, Opt. Exp. 11, 1418 (2003)
  - [13] S. Mischeau, Z. Chen, A. T. Le, J. Rauschenberger, M. F. Kling, and C. D. Lin, Phys. Rev. Lett. 102, 073001 (2009)
  - [14] S. Mischeau, Z. Chen, T. Morishita, A. T. Le, and C. D. Lin, J. Phys. B: At. Mol. Opt. Phys. 42, 065402 (2009)
  - [15] G. G. Paulus, F. Lindner, H. Walther, A. Baltuška, E. Goulielmakis, M. Lezius, and F. Krausz, Phys. Rev. Lett. 91, 253004 (2003)
  - [16] M. F. Kling, J. Rauschenberger, A. J. Verhoef, E. Hasović, T. Uphues, D. B. Milošević, H. G. Muller, and M. J. J. Vrakking, New J. Phys. 10, 025024 (2008)
  - [17] Z. Chen, T. Wittmann, B. Horvath, and C.D. Lin, Phys. Rev. A 80, 061402(R) (2009)
  - [18] T. Wittmann, B. Horvath, W. Helml, M. G. Schätzel, X. Gu, A. L. Cavalieri, G. G. Paulus, and R. Kienberger, Nature Physics 5, 357(2009)
  - [19] A. M. Sayler, M. Arbeiter, S. Fasold, D. Adolph, M. Möller, D. Hoff, T. Rathje, B. Fetić, D. B. Milošević, T. Fennel, and G. G. Paulus Opt. Lett. 40, 3137 (2015)
  - [20] Jeffrey L. Krause, Kenneth J. Schafer, and Kenneth C. Kulander, Phys. Rev. A 45, 4998(1992)
  - [21] M. Lewenstein, Ph. Balcou, M. Yu. Ivanov, Anne LHuillier, and P. B. Corkum, Phys. Rev. A 49, 2117 (1994)
  - [22] M. Lewenstein, K. C. Kulander, K. J. Schafer, and P. H. Bucksbaum, Phys. Rev. A 51, 1495(1995)
  - [23] Z. Chen, A. T. Le, T. Morishita, and C.D. Lin, Phys. Rev. A 79, 033409 (2009)
  - [24] Z. Chen, A. T. Le, T. Morishita, and C.D. Lin, J. Phys.

- B: At. Mol. Opt. Phys. 42, 061001 (2009)
- [25] T. Morishita, A. T. Le, Z. Chen, and C.D. Lin, Phys. Rev. Lett. 100, 013903 (2008)
  - [26] D. L. Carroll, FORTRAN genetic algorithm driver, 1999, <http://cuaerospace.com/carroll/ga.html> (accessed in May 2008); in *Developments in Theoretical and Applied Mechanics XVIII*, edited by H. Wilson, R. Batra, C. Bert A. Davis, R. Schapery, D. Stewart, and F. Swinson (School of Engineering, The University of Alabama, Tuscaloosa, 1996), pp. 411C424.
  - [27] J. Xu, H. L. Zhou, Z. Chen, and C. D. Lin, Phys. Rev. A 79, 052508 (2009)
  - [28] K. J. Schafer, Baorui Yang, L. F. DiMauro, and K. C. Kulander, Phys. Rev. Lett. 70, 1599 (1993)